Annals of Botany **128**: 31–44, 2021
doi: 10.1093/aob/mcab032, available online at www.academic.oup.com/aob

ANNALS OF BOTANY
Founded 1887

PART OF A FOCUS ISSUE ON ROOT BIOLOGY

Above- and below-ground resource acquisition strategies determine plant species responses to nitrogen enrichment

Dianye Zhang[1,2], Yunfeng Peng[1], Fei Li[1,2], Guibiao Yang[1,2], Jun Wang[1,2], Jianchun Yu[1,2], Guoying Zhou[3] and Yuanhe Yang[1,2,*]

[1]State Key Laboratory of Vegetation and Environmental Change, Institute of Botany, Chinese Academy of Sciences, Beijing 100093, China, [2]University of Chinese Academy of Sciences, Beijing 100049, China, and [3]Key Laboratory of Tibetan Medicine Research, Northwest Institute of Plateau Biology, Chinese Academy of Sciences, Xining 810008, China
**For correspondence. E-mail yhyang@ibcas.ac.cn*

Received: 16 September 2020 Returned for revision: 18 February 2021 Editorial decision: 19 February 2021 Accepted: 23 February 2021
Electronically published: 25 February 2021

• **Background and Aims** Knowledge of plant resource acquisition strategies is crucial for understanding the mechanisms mediating the responses of ecosystems to external nitrogen (N) input. However, few studies have considered the joint effects of above-ground (light) and below-ground (nutrient) resource acquisition strategies in regulating plant species responses to N enrichment. Here, we quantified the effects of light and non-N nutrient acquisition capacities on species relative abundance in the case of extra N input.
• **Methods** Based on an N-manipulation experiment in a Tibetan alpine steppe, we determined the responses of species relative abundances and light and nutrient acquisition capacities to N enrichment for two species with different resource acquisition strategies (the taller *Stipa purpurea*, which is colonized by arbuscular mycorrhizal fungi, and the shorter *Carex stenophylloides*, which has cluster roots). Structural equation models were developed to explore the relative effects of light and nutrient acquisition on species relative abundance along the N addition gradient.
• **Key Results** We found that the relative abundance of taller *S. purpurea* increased with the improved light acquisition along the N addition gradient. In contrast, the shorter *C. stenophylloides*, with cluster roots, excelled in acquiring phosphorus (P) so as to elevate its leaf P concentration under N enrichment by producing large amounts of carboxylate exudates that mobilized moderately labile and recalcitrant soil P forms. The increased leaf P concentration of *C. stenophylloides* enhanced its light use efficiency and promoted its relative abundance even in the shade of taller competitors.
• **Conclusions** Our findings highlight that the combined effects of above-ground (light) and below-ground (nutrient) resources rather than light alone (the prevailing perspective) determine the responses of grassland community structure to N enrichment.

Key words: Nitrogen enrichment, light acquisition, phosphorus acquisition, cluster root, root exudation, community structure.

INTRODUCTION

The amount of reactive nitrogen (N) input to terrestrial ecosystems has dramatically increased over time due to intensified human activities (e.g. agricultural fertilization) and continuous atmospheric N deposition (Galloway *et al.*, 2008). Reactive N enrichment can directly affect ecosystem functions such as gross primary productivity and the carbon (C) cycle by altering plant physiology and soil biogeochemistry (Manning *et al.*, 2006; Zhang *et al.*, 2019). Indirectly, external N input-induced changes in community structure, such as altered community composition and decreased species diversity, can also mediate the trajectories of ecosystem functions under N enrichment (Manning *et al.*, 2006). Considering that the indirect effects of reactive N inputs on community structure might even dominate ecosystem responses (Hooper *et al.*, 2012), our knowledge of the dynamics of community structure and the associated mechanisms is crucial for accurately predicting the responses of ecosystem functions to N enrichment.

During the last few decades, many studies have been conducted to investigate the effects of external N inputs on community structure and composition as well as the underlying mechanisms (Hautier *et al.*, 2009; Borer *et al.*, 2014; Dickson *et al.*, 2014; DeMalach *et al.*, 2017; Tian *et al.*, 2020). These studies highlighted that aggravated light competition was the primary driver of the contrasting responses of various species to N enrichment (Dickson *et al.*, 2014; DeMalach *et al.*, 2017; Xiao *et al.*, 2021). Considering that light is a unidirectional (decay from the top of the canopy to the bottom) and size-asymmetrical (taller individuals receive more light per unit of size than shorter individuals) resource (Onoda *et al.*, 2014), N inputs would favour tall species, as they can compete for light effectively (Tilman, 1987; Dickson *et al.*, 2014; Gross and Mittelbach, 2017). Meanwhile, the light deficiency induced by the shadow of tall species would suppress the biomass and richness of short species (Dickson *et al.*, 2014; DeMalach *et al.*, 2017). However, none of these studies has quantified the amount of light acquired by various species, which leaves unexplored

the fundamental linkages between the responses of species relative abundance to N enrichment and plant light acquisition capacity. Moreover, N-induced increases in leaf area and specific leaf area (Zhang *et al.*, 2019) would also favour light acquisition by short species even when being shaded by their taller competitors (Hirose and Werger, 1995; Kohyama and Takada, 2009; Onoda *et al.*, 2014). For this reason, the accurate quantification of the amount of light acquired by various species is essential for better exploring the mechanisms underlying the fates of various species under N enrichment.

Apart from increasing light acquisition, plants would cope with N-induced light competition by altering their acquisition of non-N nutrients [e.g. phosphorus (P) and some micronutrients] due to the strong regulation of light use efficiency by leaf nutrient status (Wright *et al.*, 2004). However, few studies have focused on the different trajectories of leaf non-N nutrient concentrations among different species under N input. Taking leaf P concentration as an example, the prevailing perspective suggests that leaf P concentration would decline under external N input due to the imbalance between the N-induced increase in plant P demand and the elevated soil P supply as a result of the enhancement of root and soil phosphatase activity (Li *et al.*, 2016; Deng *et al.*, 2017). In addition to secreting phosphatase, plants could also acquire P by altering their P resorption, mycorrhizal colonization, root morphology, root vitality, root carboxylate exudation and utilization of different soil P fractions (Shen *et al.*, 2011; Lambers *et al.*, 2015; Yu *et al.*, 2020). More importantly, these P acquisition strategies could allow some species (e.g. plants with cluster roots) to acquire P effectively even under P-poor conditions (Vance *et al.*, 2003) and further induce different responses to N enrichment in the leaf P concentrations of various species. However, to date few studies have quantified the differences in these nutrient acquisition strategies among species and considered the combined effects of above-ground (light) and below-ground (nutrients) resource acquisition in regulating the responses of species relative abundance to N enrichment.

To fill this knowledge gap, we explored the effects of N input on species relative abundance, light acquisition and leaf nutrient concentrations of two species with different resource acquisition strategies [the taller, dominant species *Stipa purpurea*, which is colonized by arbuscular mycorrhizal fungi (AMF), and the shorter subordinate species *Carex stenophylloides*, which has cluster roots] and quantified the linkages between species relative abundance and above-/below-ground resource acquisition in a Tibetan alpine steppe. We also examined the relationship between species relative abundance and resource acquisition for two extra species (subordinate species *Poa poophagorum* and subordinate species *Potentilla multifida*) whose relative abundance declined under N enrichment. To further investigate the drivers of the contrasting resource acquisition trends of *S. purpurea* and *C. stenophylloides*, we measured a series of plant and soil parameters, including plant height, leaf and root morphology, mycorrhizal colonization, root vitality, root extracellular enzyme activity, root carboxylate exudation, leaf nutrient resorption efficiency and rhizosphere soil nutrient status. The aim of our study was to explore the mechanisms underlying the species-specific responses of plant relative abundance to N enrichment. We hypothesized that above-ground (light) and below-ground (nutrients) resource acquisition would co-determine the effects of N input on species relative abundance. Specifically, plants would invest additional N in shoot growth and further acquire more light. Species relative abundance would then increase with the improved light acquisition. Meanwhile, both *S. purpurea* (colonized by AMF) and *C. stenophylloides* (with cluster roots) might alter their nutrient acquisition traits (e.g. synthesizing and secreting more phosphatase and carboxylates) to take up more non-N nutrients and thus enhance leaf nutrient concentrations. The increased leaf nutrient concentrations would then promote species relative abundance, even under a strong light competition scenario.

MATERIALS AND METHODS

Site description and experimental design

The study was carried out in an alpine steppe (37°18′ N, 100°15′ E; 3290 m a. s. l.) located on the north-eastern Tibetan Plateau, China. The study site experiences an alpine continental climate in which cold and dry winters alternate with relatively warm and wet summers. The mean annual temperature is 0.08 °C, with average precipitation of ~390 mm, falling predominantly in May–September. The local vegetation is composed of the dominant species (relative abundance >20 %; Ye *et al.*, 2018) *Stipa purpurea*, subordinate species (relative abundance between 1 % and 20 %; Sánchez-Castillo *et al.*, 2008), including *Carex stenophylloides*, *Poa poophagorum*, *Leymus secalinus*, *Agropyron cristatum*, *Potentilla multifida* and *Heteropappus altaicus*, and several rare species (relative abundance <1 %; Mouillot *et al.*, 2013), including *Dracocephalum heterophyllum*, *Leontopodium nanum* and *Potentilla bifurca*. The soil type is a Haplic Calcisol according to the FAO classification system, with 11.6 ± 3.6 mg kg^{-1} of inorganic N (extracted by 1 M KCl) and 2.2 ± 0.3 mg kg^{-1} of Olsen-P (labile inorganic P extracted by 0.5 M $NaHCO_3$) in the top 30 cm of soil (Peng *et al.*, 2017). This alpine steppe was historically used as a winter pasture for sheep, and no additional management practices (such as fertilization or irrigation) were applied before our experiment.

We fenced the experimental field (0.5 ha) and established the N manipulation experiment in May 2013. The experiment was set in a randomized complete block design, with five blocks (isolated by buffer zones of 2 m) and eight N treatments (0, 1, 2, 4, 8, 16, 24 and 32 g N m^{-2} $year^{-1}$). The N treatments ranged from N limitation to N saturation, which may occur at ~15 g N m^{-2} $year^{-1}$ in grassland ecosystems around the world (Peng *et al.*, 2020). Considering that the N saturation threshold appears to be ecosystem-dependent [e.g. the results from an alpine meadow on the Tibetan Plateau showed that below-ground net primary productivity first increased and then decreased at 2–4 g N m^{-2} $year^{-1}$ (Wang *et al.*, 2019), while the addition of 10 g N m^{-2} $year^{-1}$ had a weak effect on most functional traits in Konza Prairie (La Pierre and Smith, 2015)], we established this N addition gradient (eight N levels up to 32 g N m^{-2} $year^{-1}$) to ensure that non-linear responses would be included and that the saturation threshold would be detected. In each block, the eight N addition levels were randomly assigned to 6 × 6-m^2 plots (isolated by buffer zones of 1 m). The N fertilizer applied

to a targeted plot was divided into five equal parts, and each part was dissolved in 10 L of water and evenly sprinkled on the corresponding plot at the beginning of each month during the growing season (May to September). Each control plot also received 10 L of water without N. The confounding effect of water addition could be ignored since it was equivalent to an addition of only 1.5 mm year^{-1} of rainfall and accounted for ~0.4 % of the annual precipitation (Zhang *et al.*, 2019).

Species relative abundance, light acquisition and leaf nutrient concentration measurements

The relative abundances of *S. purpurea*, *C. stenophylloides*, *P. poophagorum* and *P. multifida* were determined in mid-August 2016. Specifically, we recorded the species richness and the number of individuals per species (i.e. the abundance of the targeted species) based on a permanent 1 × 1-m^2 quadrat. The species relative abundance was then calculated as the ratio of the number of individuals of a species to the number of individuals within the quadrat.

To quantify the light acquisition of *S. purpurea*, *C. stenophylloides*, *P. poophagorum* and *P. multifida*, we divided the canopy into several layers (equal to the number of species) according to the maximum vegetative height of the different species in each plot (Supplementary Data Fig. S1A). We then calculated the amount of photosynthetically active radiation (PAR; 400–700 nm waveband) acquired by each species using the following formula (Anten and Hirose, 1999; Kamiyama *et al.*, 2010):

$$PAR_i = \sum_{j}^{n} PAR_{ij}$$

where PAR_i is the amount of PAR acquired by species i in the whole canopy (μmol photons m^{-2} s^{-1}), PAR_{ij} is the PAR acquired by species i in layer j (μmol photons m^{-2} s^{-1}) and n is the number of layers (i.e. the number of species). PAR_{ij} was quantified using the following equation (Hirose and Werger, 1995; Anten and Hirose, 1999; Kamiyama *et al.*, 2010):

$$PAR_{ij} = PAR_j \times (LA_{ij} / \sum_{i}^{s} LA_{ij})$$

where PAR_j is the PAR absorbed by layer j (μmol photons m^{-2} s^{-1}), LA_{ij} is the leaf area of species i in layer j (cm^2) and s is the number of species existing in layer j. To estimate LA_{ij}, all plants in three 0.25 × 0.25-m^2 quadrats were harvested and sorted by individual species. The harvested plant materials for each species were cut into several segments starting at the base. The species with a maximum height taller than 15 cm were cut into 5-cm segments and the other species were cut into 2-cm segments (Hirose and Werger, 1995; Anten and Hirose, 1999). The total leaf area of each segment was measured for each species, and empirical functions of the relationship between leaf area and height of the segments were established for the target species (Ramesh *et al.*, 2007). Then, LA_{ij} was estimated on the basis of the established empirical function and the height of layer j for species i. PAR_j can be estimated according to the intercepted and reflected PAR in layer j (Supplementary Data Fig. S1B; Tagesson *et al.*, 2015):

$$PAR_j = PAR_{inc,j} - PAR_{inc,j+1} - PAR_{ref,j} + PAR_{ref,j+1}$$

where $PAR_{inc,j}$ is the incoming PAR to layer j (μmol photons m^{-2} s^{-1}) and PAR_{ref} is the PAR reflected by layer j (μmol photons m^{-2} s^{-1}).

To obtain the incoming and reflected PAR for a given layer, we measured these values at eight heights (0, 5, 10, 20, 40, 60, 80 and 100 cm) in each plot using a canopy analyser [an analyser with a linear light ceptometer (50 cm length × 2 cm width × 2 cm height); Top-1000; Zhejiang Top Instrument, Hangzhou, Zhejiang, China]. The PAR measurements were taken between 11:00 a.m. and 14:00 p.m. on a sunny and cloudless day in mid-August, with ten repetitions in each plot. We then quantified the association between the observed PAR and canopy height according to the following light decay equation (Supplementary Data Fig. S1C; Anten and Hirose, 1999; DeMalach *et al.*, 2017):

$$\log(PAR) = a \times \ln(H) + b$$

where PAR is the incoming or reflected PAR (μmol photons m^{-2} s^{-1}) and H is the canopy height (cm). Finally, we calculated the incoming and reflected PAR for the specific layers based on the light decay equation and the height of the layer in each plot.

For the leaf nutrient concentrations of *S. purpurea*, *C. stenophylloides*, *P. poophagorum* and *P. multifida*, we measured the leaf P, potassium (K), calcium (Ca), sodium (Na), magnesium (Mg), aluminium (Al), copper (Cu), iron (Fe), manganese (Mn) and zinc (Zn) concentrations because N addition can aggravate plant non-N nutrient limitation (Li *et al.*, 2016). Specifically, the non-N nutrient concentrations of the leaves were measured by inductively coupled plasma atomic emission spectroscopy (ICAP6300, Thermo Fisher Scientific, Waltham, MA, USA) after digesting the leaf samples with acid. In addition, the leaf N concentration was determined using an elemental analyser (Vario EL III, Elementar, Germany).

Plant resource acquisition trait measurements

For the plant light acquisition traits, we measured the plant height, leaf area and specific leaf area (a large plant size and specific leaf area can promote plant light acquisition; Pérez-Harguindeguy *et al.*, 2013; Laurans and Vincent, 2016). Specifically, we measured 20 healthy and mature individuals to obtain the vegetative height for *S. purpurea* and *C. stenophylloides* in the field and then harvested the leaves of these individuals. The collected leaves were scanned and analysed by WinFOLIA software (Regent Instruments, Quebec City, Quebec Canada) to determine their leaf area, and oven-dried to obtain their leaf weight. The specific leaf area was calculated as the ratio of leaf area to leaf weight (Pérez-Harguindeguy *et al.*, 2013). For details of the procedure for measuring light acquisition traits see Zhang *et al.* (2019).

For the plant nutrient acquisition traits, we measured mycorrhizal colonization, specific root length, root vitality (plants with higher mycorrhizal colonization, specific root length and root vitality can take up more soluble inorganic nutrients from the soil; Shen *et al.*, 2011; Treseder, 2013), root phosphomonoesterase (PME) activity and root

carboxylate exudation (plants can secrete PME to hydrolyse soluble organic nutrients and carboxylates to mobilize insoluble nutrient forms; thus, exuding more PME and carboxylates can increase the soil available nutrient supply; Marklein and Houlton, 2012; Lambers *et al.*, 2015). Specifically, we excavated the roots from the top 0–10 cm of soil at five random locations within each plot. The collected root samples within each plot were mixed and classified as *S. purpurea*, *C. stenophylloides* or other species by their morphological characteristics. Then, the root samples of *S. purpurea* and *C. stenophylloides* were classified into different orders, with the most distal root tips being termed the first order (Xia *et al.*, 2010). We chose to measure root P acquisition traits of the first three orders of roots since they are closely related to plant nutrient uptake (McCormack *et al.*, 2015).

After root sampling, mycorrhizal colonization was measured using the trypan blue staining technique (Johnson *et al.*, 2003). Briefly, fresh roots were cleared with KOH solution, bleached with alkaline H_2O_2 and soaked in an acid solution. The acidified roots were stained in acidic trypan blue solution, destained in acidic glycerol and then used to estimate mycorrhizal colonization. Specific root length refers to the ratio of root length to root weight (Pérez-Harguindeguy *et al.*, 2013). The rinsed roots were scanned and analysed with WinRHIZO software (Regent Instruments, Quebec City, Quebec, Canada) to measure their root length. Then, the samples were oven-dried and weighed to determine their specific root length. Root vitality was measured using the triphenyltetrazolium chloride (TTC) reduction method (Comas *et al.*, 2000). For the TTC reduction test, ~500 mg of rinsed roots was soaked in TTC buffer solution, vacuum-infiltrated, and subsequently incubated for 24 h in the dark. During the thermostatic incubation (25 °C), colourless TTC was reduced to red triphenyl-formazan. The amount of TTC reduction, which is proportional to root vitality, was then determined with a spectrophotometer (UV-2550, Shimadzu, Kyoto, Japan) at 490 nm.

Root carboxylate (citrate and malate) exudation was measured with a citric acid assay kit (K-CITR, Megazyme, Wicklow, Ireland) and a malic acid assay kit (K-LMALQR, Megazyme, Wicklow, Ireland) following the manufacturer's protocols. The citric acid assay kit quantified citrate according to the oxidation of nicotinamide adenine dinucleotide (NADH), while the malic acid assay kit determined malate by the formation of NADH (Dinkelaker *et al.*, 1989; Kabir *et al.*, 2013). The changes in NADH were determined with a spectrophotometer (UV-2550, Shimadzu, Kyoto, Japan) at 340 nm. Root PME activity was determined according to microplate fluorometric technology (Marx *et al.*, 2001). First, we soaked ~200 mg of rinsed roots in 50 mL of Tris-buffer solution and incubated them for 1 h at 25 °C. Subsequently, 200 µL of root-extracted solution was placed in a 96-well microplate and mixed with 50 µL of 4-methylumbelliferone-linked phosphate, and the mixture was incubated for 2 h at 25 °C in the dark. After incubation, the fluorescence of each sample, which is proportional to the PME activity, was determined with an automatic microplate reader (DTX 880 Multimode Detector, Beckman Coulter, Fullerton, CA, USA) with 365-nm excitation and 450-nm emission wavelengths.

We also measured the plant nutrient resorption efficiency (Vergutz *et al.*, 2012) and root:shoot ratio (Gedroc *et al.*, 1996), which are closely associated with plant nutrient acquisition. Phosphorus resorption efficiency was calculated according to the following equation (Vergutz *et al.*, 2012):

$$\text{P resorption efficiency} = (1 - P_i/P_g \times \text{MLCF}) \times 100$$

where P_g is the P concentration of mature green leaf (mg g^{-1}; sampled in mid-August), P_i is the P concentration of fresh leaf litter (mg g^{-1}; sampled in late October) and MLCF is the mass loss correction factor (the MLCFs of *S. purpurea* and *C. stenophylloides* are considered to be 0.713 and 0.640, respectively; Vergutz *et al.*, 2012). The root:shoot ratios for *S. purpurea* and *C. stenophylloides* were calculated as the ratio of the root biomass in the top 30 cm of soil to the corresponding above-ground biomass.

We further determined the rhizosphere soil P fractions using the sequential P fractionation method (Hedley *et al.*, 1982; Tiessen and Moir, 1993). Rhizosphere soil collection was performed at the same time as the root sampling; we collected the soil that was still adhered to the roots after gently shaking the roots (Marilley *et al.*, 1998). The soil samples were air-dried and analysed by the sequential extraction method (resin extraction followed by 0.5 M $NaHCO_3$ extraction, 0.1 M NaOH extraction and 1 M HCl extraction) to extract labile resin-inorganic P (Pi), $NaHCO_3$-Pi and $NaHCO_3$-organic P (Po); moderately labile NaOH-Pi and NaOH-Po; and recalcitrant HCl-Pi (Hedley *et al.*, 1982; Tiessen and Moir, 1993). The Pi in the extractant was measured using the ammonium molybdate method, and Po was calculated as the difference between the total P (determined by inductively coupled plasma atomic emission spectroscopy) and Pi. In addition, we measured the rhizosphere soil-available micronutrients (Cu, Fe, Mn, Zn) using inductively coupled plasma atomic emission spectroscopy after extracting soil samples according to the diethylenetriaminepentaacetic acid procedure (Lindsay and Norvell, 1978).

Statistical analyses

We analysed the data with the following three steps. First, one-way ANOVAs were used to explore the effects of N enrichment on species relative abundance, plant resource acquisition (plant PAR acquisition, leaf nutrient concentration), plant traits, and rhizosphere soil nutrient status. During these analyses, the N addition level was assigned as a fixed factor, and the block was assigned as a random factor (because the effects of the block were caused by heterogeneity; Dutilleul, 1993). Subsequently, *post hoc* analyses (Tukey's honestly significant difference test; Hothorn *et al.*, 2008) were conducted to examine the differences among treatments for those variables that exhibited significant changes along the N gradient.

Second, linear mixed-effects regression models were used to identify the drivers of species relative abundance under extra N input. Specifically, we examined the single-variable relationships of species relative abundance with resource acquisition based on linear mixed-effects regression models. During these analyses, resource acquisition was treated as a fixed factor and

the block was treated as a random factor. Subsequently, single-variable linear mixed-effects regression models were developed to examine the relationships of resource acquisition to plant resource acquisition traits and rhizosphere soil nutrient status. In these linear mixed-effects models, plant traits and rhizosphere soil nutrient status were treated as fixed factors and the block was treated as a random factor. All residuals of the models were tested for homoscedasticity and normality. The ANOVAs and linear mixed-effects models were performed using the lme4 package (Bates *et al.*, 2015) in R 3.6.0 (R Core Team, 2019).

Third, structural equation models were used to explore the relative effects of the predictors on species relative abundance. In the initial structural equation model, the N addition level was considered as an exogenous variable; plant resource acquisition, plant traits and rhizosphere soil nutrient status were set as the endogenous variables; and species relative abundance was the final response variable (Supplementary Data Fig. S2). Then, iterative model optimization was performed to improve the goodness of fit of the model. Fisher's *C* statistic, Akaike's information criterion corrected for small sample size (AICc) and the whole-model *P* value were used to evaluate the model performance (Lefcheck, 2016). Lower Fisher *C* and AICc values and higher *P* values (>0.05) reflected a better-fitting model (Lefcheck, 2016). The structural equation models were conducted using the piecewiseSEM package in R 3.6.0 (R Core Team, 2019) with the block as the random effect. Notably, as some plant relative abundance and light acquisition parameters showed unimodal responses to N addition with a threshold of 8 g N m^{-2} $year^{-1}$, we divided the corresponding data into two parts (≤8 g N m^{-2} $year^{-1}$, low N; and >8 g N m^{-2} $year^{-1}$, high N) and conducted the linear mixed-effects regression model and structural equation model under the low-N and high-N treatments, respectively.

RESULTS

Nitrogen-induced changes in species relative abundance, resource acquisition, plant traits and rhizosphere soil nutrient status

Our results showed that species relative abundance, PAR acquisition and leaf P and micronutrient concentrations showed different responses to N enrichment (Fig. 1; Supplementary Data Table S1). Specifically, along the N addition gradient, the relative abundance and PAR acquisition of the dominant species *S. purpurea* increased (all $P < 0.05$; Fig. 1A, B),

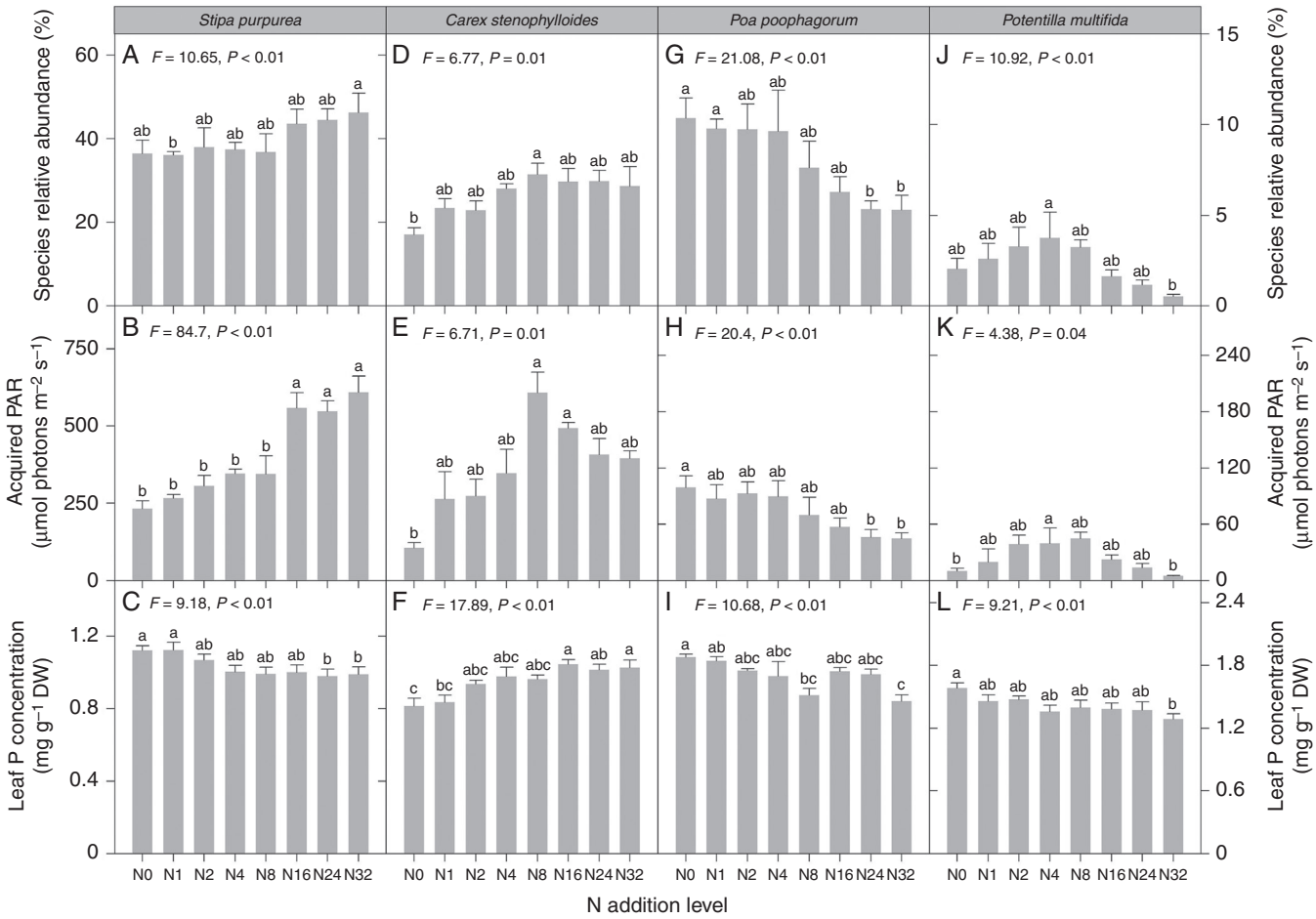

FIG. 1. Changes in species relative abundance, light acquisition and leaf P concentration along the experimental N gradient. Values are means ± s.e. ($n = 5$), and the same letter denotes a non-significant difference among N treatments ($P > 0.05$). DW, dry weight; N0, N1, N2, N4, N8, N16, N24 and N32 represent N addition rates of 0, 1, 2, 4, 8, 16, 24 and 32 g N m^{-2} $year^{-1}$, respectively.

while its leaf P concentration declined ($P < 0.05$; Fig. 1C). For *C. stenophylloides*, relative abundance almost doubled ($P < 0.05$; Fig. 1D) and leaf P and micronutrient (Cu, Mn and Zn) concentrations increased along the N addition gradient (all $P < 0.05$; Fig. 1F; Supplementary Data Table S1); PAR acquisition showed a unimodal response to N enrichment with a threshold of 8 g N m^{-2} $year^{-1}$ (Fig. 1E). For *P. poophagorum*, relative abundance, PAR acquisition and leaf P concentration all declined along the experimental N addition gradient (all $P < 0.05$; Fig. 1G–I). For *P. multifida*, relative abundance and PAR acquisition exhibited hump-shaped responses to N enrichment (all $P < 0.05$; Fig. 1J, K), while leaf P concentration declined along the N addition gradient ($P < 0.05$; Fig. 1L).

In terms of light acquisition traits, the plant height, leaf area and specific leaf area of *S. purpurea* and *C. stenophylloides* all increased along the experimental N addition gradient (all $P < 0.05$; Fig. 2). For nutrient acquisition traits, the mycorrhizal colonization of *S. purpurea* decreased, while the root vitality, root phosphatase activity and root carboxylate exudation of *S. purpurea* and *C. stenophylloides* increased along the N addition gradient (all $P < 0.05$; Fig. 3A, C–E; the results are shown separately for citrate and malate in Supplementary Data Fig. S3). Moreover, the root:shoot ratio of *C. stenophylloides* declined under N enrichment ($P < 0.05$; Supplementary Data Fig. S4), while the specific root length and P resorption efficiency of *S. purpurea* and *C. stenophylloides* remained stable (Fig. 3B, F). In terms of the rhizosphere soil P fraction, N enrichment significantly reduced the resin-Pi, $NaHCO_3$-Pi and $NaHCO_3$-Po of *S. purpurea* rhizosphere soil (all $P < 0.05$; Table 1). The NaOH-Pi, NaOH-Po and HCl-Pi of *C. stenophylloides* rhizosphere soil decreased under N enrichment (all $P < 0.05$; Table 1). For rhizosphere soil micronutrient availability, N enrichment significantly decreased the rhizosphere soil Cu, Fe, Mn and Zn availability for both *S. purpurea* and *C. stenophylloides* (all $P < 0.05$; Supplementary Data Table S2).

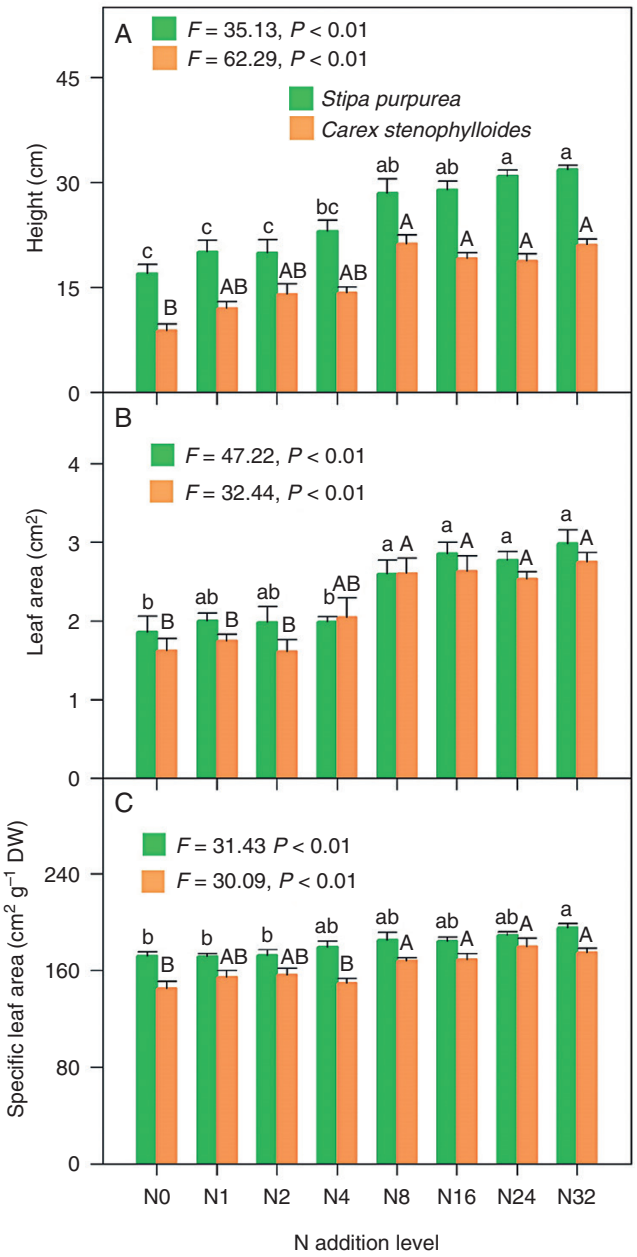

FIG. 2. Responses of light acquisition traits of *S. purpurea* and *C. stenophylloides* to N enrichment. Values are means ± s.e. ($n = 5$). Capital and lowercase letters above bars denote differences between treatments for *S. purpurea* and *C. stenophylloides*, respectively, and the same letter represents a non-significant difference among N treatments ($P > 0.05$). DW, dry weight; N0, N1, N2, N4, N8, N16, N24 and N32 represent N addition rates of 0, 1, 2, 4, 8, 16, 24 and 32 g N m^{-2} $year^{-1}$, respectively.

Linkages between species relative abundance and resource acquisition, plant traits and rhizosphere soil nutrient status

Our results indicated that the relative abundances of *S. purpurea*, *P. poophagorum* and *P. multifida* exhibited positive correlations with plant PAR acquisition under both low and high N levels (all $P < 0.05$; Fig. 4A, E, G). Moreover, although the leaf P concentration was positively correlated with the relative abundance for *P. poophagorum* under both low and high N levels, and for *P. multifida* under high N levels, it exhibited negative correlations with the relative abundance for *S. purpurea* and *P. multifida* under low N levels (all $P < 0.05$; Fig. 4B, F, H). For *C. stenophylloides*, relative abundance was positively correlated with both plant PAR acquisition and leaf nutrient (P, Mn and Zn) concentrations under low N levels (all $P < 0.05$; Fig. 4C, D; Supplementary Data Fig. S5B, C). However, under high N levels, the relative abundance of *C. stenophylloides* exhibited positive correlations only with leaf nutrient (P, Mn and Zn) concentrations ($P < 0.05$; Fig. 4D; Supplementary Data Fig. S5B, C).

Our results also revealed that the PAR acquisition of *S. purpurea* and *C. stenophylloides* was closely associated with plant height and leaf area (all $P < 0.05$; Fig. 5A, B). The leaf P concentration of *S. purpurea* showed a positive relationship with mycorrhizal colonization under low N levels, and decreased with increasing root vigour, root phosphatase activity and root carboxylate exudation along the entire N gradient (all $P < 0.05$; Fig. 5A). However, leaf P concentration of *C. stenophylloides* exhibited positive associations with root vigour, root phosphatase activity and root carboxylate

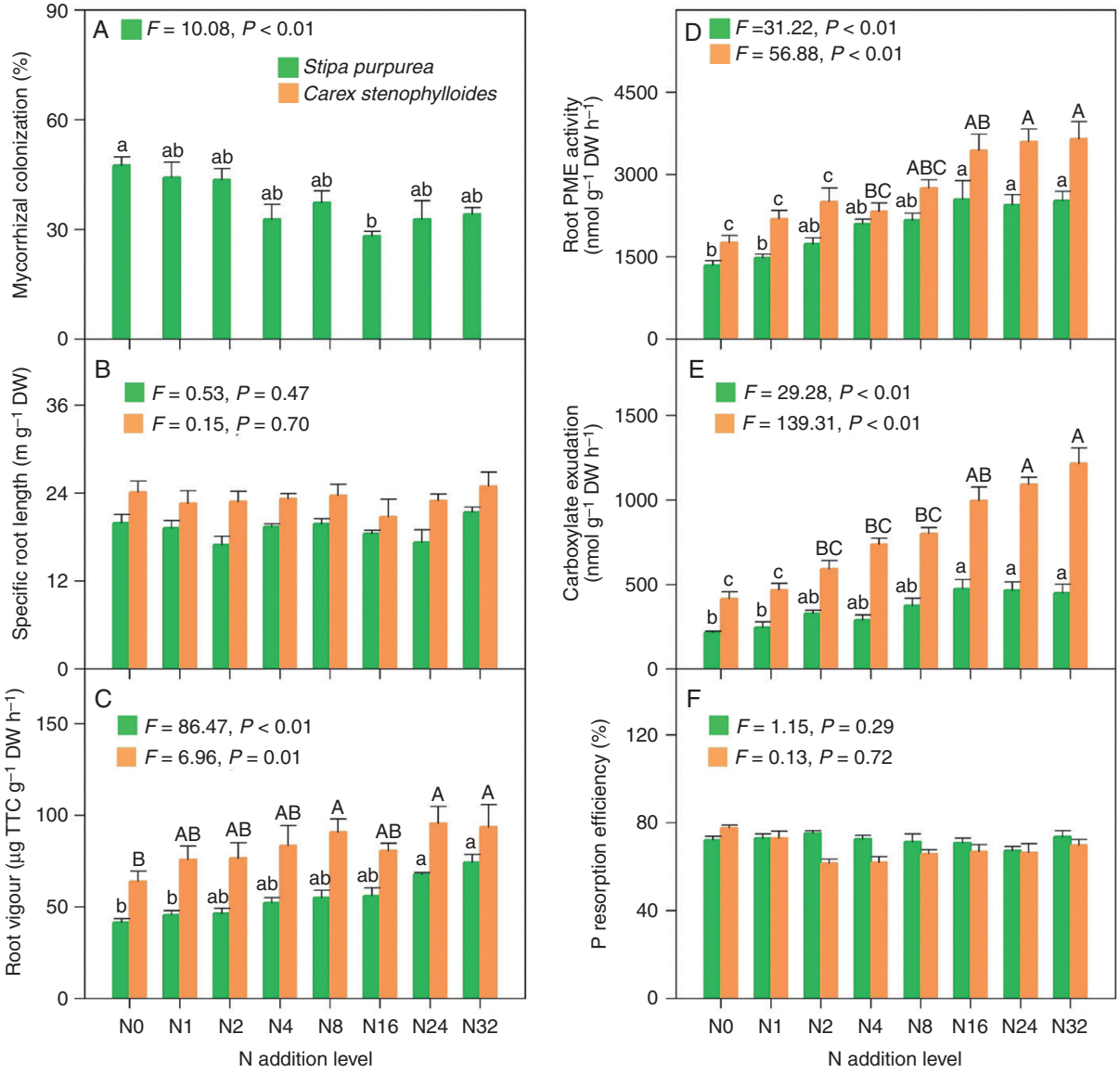

FIG. 3. Responses of nutrient acquisition traits of *S. purpurea* and *C. stenophylloides* to N enrichment. Values are means ± s.e. ($n = 5$). Capital and lowercase letters above bars denote differences between treatments for *S. purpurea* and *C. stenophylloides*, respectively, and the same letter represents a non-significant difference among N treatments ($P > 0.05$). Because *C. stenophylloides* is a non-mycorrhizal plant, we only show mycorrhizal colonization of *S. purpurea* in panel (A). DW, dry weight; N0, N1, N2, N4, N8, N16, N24 and N32 represent N addition rates of 0, 1, 2, 4, 8, 16, 24 and 32 g N m^{-2} $year^{-1}$, respectively.

exudation, and negative correlations with the moderately labile (NaOH-Pi and NaOH-Po) and recalcitrant (HCl-Pi) fractions in rhizosphere soil (all $P < 0.05$; Fig. 5B). In addition, the leaf micronutrient concentration of *C. stenophylloides* showed a positive relationship with root carboxylate exudation ($P < 0.05$; Supplementary Data Fig. S6).

Further analyses demonstrated that light was the dominant factor driving the response of the relative abundance of *S. purpurea* to N enrichment (Fig. 6A, B). Acquisition of PAR could explain 57 and 75 % of the variation in the relative abundance of *S. purpurea* at low N and high N levels, respectively. For *C. stenophylloides*, PAR acquisition and leaf P concentration co-determined the response of relative abundance under low N levels (Fig. 6C). However, the increased leaf P concentration induced by increased carboxylate exudation was the most important driver of the relative abundance of *C. stenophylloides* under high N levels (Fig. 6D). The combination of the leaf P concentration and carboxylate exudation explained 59 % of the variation in the relative abundance of *C. stenophylloides* under high N levels.

DISCUSSION

Based on the quantification of above-ground (light) and below-ground (P and other non-N nutrients) resources acquired by specific species, this study provided the first evidence that light and nutrients co-drove the response of plant species to N enrichment (Fig. 7). Specifically, structural equation model and stepwise regression analyses (Supplementary Data Table S3) revealed that

TABLE 1. *Responses of rhizosphere soil P fractions (mg kg^{-1}) of* S. purpurea *and* C. stenophylloides *to increasing N addition*

Species	Soil P fraction	*P* value	N addition rate (g N m^{-2} year^{-1})							
			0	1	2	4	8	16	24	32
S. purpurea	Resin-Pi	<0.01	5.5 ± 0.3^{a}	5 ± 0.3^{ab}	5 ± 0.3^{ab}	5.1 ± 0.4^{ab}	4.3 ± 0.4^{abc}	3.6 ± 0.3^{bc}	3.8 ± 0.4^{bc}	2.9 ± 0.4^{c}
	$NaHCO_3$-Pi	0.04	3.4 ± 0.1^{a}	3.2 ± 0.3^{ab}	3.3 ± 0.3^{ab}	3.4 ± 0.4^{ab}	2.5 ± 0.4^{ab}	2 ± 0.3^{ab}	2.2 ± 0.3^{ab}	1.7 ± 0.2^{b}
	$NaHCO_3$-Po	<0.01	2.7 ± 0.1^{ab}	1.9 ± 0.3^{ab}	3.1 ± 0.2^{a}	3 ± 0.3^{ab}	2 ± 0.1^{b}	2.1 ± 0.2^{ab}	2.1 ± 0.2^{ab}	2.2 ± 0.1^{b}
	NaOH-Pi	0.05	14.6 ± 0.5	14.5 ± 0.8	16.7 ± 0.8	12.8 ± 0.3	14.4 ± 0.5	12.9 ± 0.8	13.8 ± 0.7	13.8 ± 0.5
	NaOH-Po	0.05	11.8 ± 0.5	9.6 ± 0.6	11 ± 0.7	10.3 ± 0.8	11.6 ± 0.9	10.8 ± 0.7	10.4 ± 0.4	10.9 ± 0.3
	HCL-Pi	0.3	65.7 ± 1.2	65.4 ± 1	65.2 ± 0.6	63.2 ± 1.6	62.8 ± 0.8	61 ± 1.1	62.7 ± 3.7	63.4 ± 2.1
C. stenophylloides	Resin-Pi	0.08	5.0 ± 0.3	5.3 ± 0.3	4.6 ± 0.5	4.3 ± 0.3	4.5 ± 0.5	4.2 ± 0.6	4.3 ± 0.5	4.2 ± 0.2
	$NaHCO_3$-Pi	0.05	2.4 ± 0.2	2.5 ± 0.1	2.4 ± 0.2	2.8 ± 0.1	2.7 ± 0.2	2.8 ± 0.2	2.8 ± 0.1	2.7 ± 0.2
	$NaHCO_3$-Po	0.88	2.6 ± 0.2	2.4 ± 0.1	2.6 ± 0.1	2.5 ± 0.2	2.6 ± 0.1	2.5 ± 0.2	2.4 ± 0.1	2.4 ± 0.2
	NaOH-Pi	<0.01	14.5 ± 1.2^{a}	14 ± 1.2^{ab}	12.7 ± 0.6^{ab}	13.3 ± 1.8^{ab}	11.8 ± 1.1^{ab}	12.4 ± 0.8^{ab}	10.9 ± 0.7^{b}	11.8 ± 0.8^{ab}
	NaOH-Po	0.04	11.3 ± 0.6^{ab}	10.5 ± 0.7^{ab}	11.5 ± 0.4^{a}	10.2 ± 0.6^{ab}	10.3 ± 1.1^{ab}	8.9 ± 0.9^{b}	9.7 ± 1.1^{ab}	8.7 ± 0.7^{b}
	HCL-Pi	<0.01	67.3 ± 1.2^{a}	63 ± 1.7^{ab}	61.5 ± 1.9^{abc}	57.7 ± 2.2^{bcd}	54.5 ± 1.2^{bcd}	54.8 ± 1.1^{bcd}	53.8 ± 2^{cd}	52.5 ± 1.1^{d}

Values displayed in the table are means ± s.e. ($n = 5$).
Values in a specific row followed by the same letter denote a non-significant difference among N treatments ($P > 0.05$).

light acquired by each species dominated the different fates of *S. purpurea*, *P. poophagorum* and *P. multifida* under N enrichment. This finding advances our understanding of the crucial role of light in shaping the complex responses (increasing, decreasing and unimodal) of plant species to N enrichment beyond the traditional perspective about the inhibition of short species by monotonously increasing community light interception (Borer *et al.*, 2014) or light asymmetry (Supplementary Data Fig. S7; DeMalach *et al.*, 2017). For *S. purpurea*, its stronger light acquisition promoted its relative abundance, while the weaker light acquisition of *P. poophagorum* induced a decrease in its relative abundance. It has been reported that light is a unidirectional and asymmetrical resource input from the top of the canopy to the bottom (Onoda *et al.*, 2014) and that N enrichment would increase light asymmetry (DeMalach *et al.*, 2017). In this study, *S. purpurea* acquired light more efficiently than other species because *S. purpurea* included tall individuals and showed increased leaf area along the N addition gradient. Meanwhile, the light acquisition of *P. poophagorum* may be suppressed by increased shading and light asymmetry (Borer *et al.*, 2014; DeMalach *et al.*, 2017); thus, its relative abundance decreased. However, for *P. multifida*, whose light acquisition showed a unimodal response to N enrichment, its relative abundance increased initially but decreased after a threshold of 8 g N m^{-2} year^{-1}. The initial increase in light acquisition at low N levels may have occurred because N enrichment could also stimulate the growth of shorter species and increase their plant height and leaf area (Zhang *et al.*, 2019), which was beneficial for light acquisition. Consequently, the relative abundance of *P. multifida* increased, especially under low N levels when the shading effect of taller species and the light asymmetry were not strong. Nevertheless, the inhibitory effect of the intensified shading exceeded the facilitation of increased plant size at high N levels, leading to decreased light acquisition and relative abundance for *P. multifida*. Overall, the quantification of light by different species, as performed in this study, offers the possibility of revealing the mechanisms underlying the species-specific responses to various N addition levels.

Our results also demonstrated that the increased leaf nutrient (especially P) concentrations of *C. stenophylloides* offset the negative effect of decreased light acquisition under high N levels, and promoted its relative abundance even in the shade of taller competitors (Fig. 6C, D). This finding agrees with our hypothesis that above- and below-ground resource acquisition strategies co-determine the response of community structure in the case of N input and does not support the previously suggested view that light itself determines species persistence under N enrichment (Hautier *et al.*, 2009; Borer *et al.*, 2014; DeMalach *et al.*, 2017). Although light competition is important in regulating community structure under N enrichment, plants would cope with light competition not only by modifying their light acquisition capacity but also by altering their light use efficiency (Anten, 2005; Onoda *et al.*, 2014). In this study, light acquisition by *S. purpurea* increased along the N addition gradient, which stimulated its relative abundance. However, for *C. stenophylloides* the light acquired initially increased but subsequently decreased at levels higher than 8 g N m^{-2} year^{-1}. Nevertheless, N enrichment improved the light use efficiency of *C. stenophylloides* (Supplementary Data Fig. S8A), and thus induced its high relative abundance at high N levels. The increased light use efficiency of *C. stenophylloides*

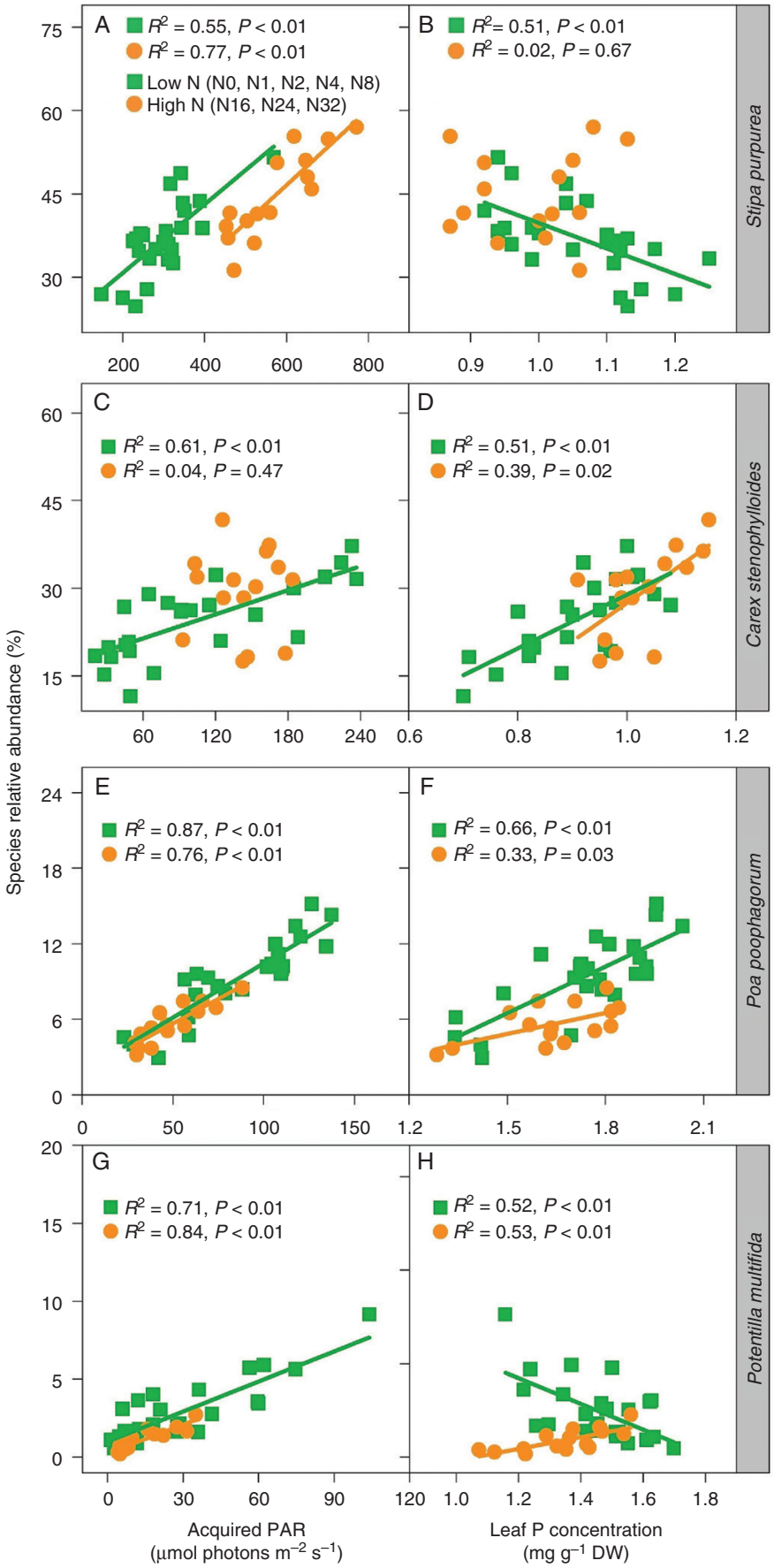

FIG. 4. Relationships of species relative abundance with light acquisition and leaf P concentration. DW, dry weight; N0, N1, N2, N4, N8, N16, N24 and N32 represent N addition rates of 0, 1, 2, 4, 8, 16, 24 and 32 g N m^{-2} year^{-1}, respectively.

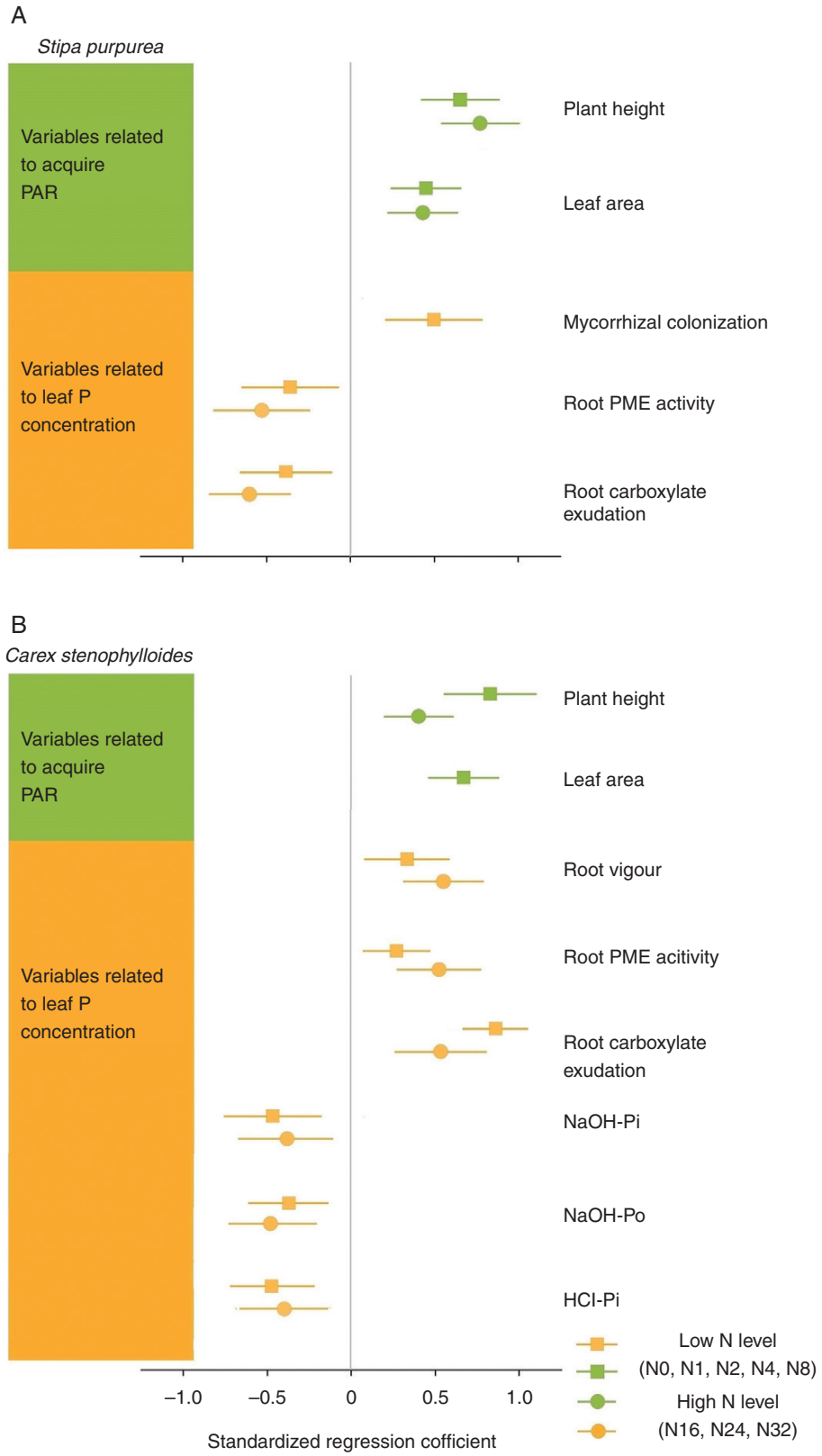

FIG. 5. Linkages of light acquisition and leaf P concentration with plant traits and rhizosphere soil P fraction for *S. purpurea* (A) and *C. stenophylloides* (B). The plant and soil parameters shown in the figure all exhibit significant effects on plant resource acquisition (all $P < 0.05$). The data points represent standardized regression coefficients obtained from single-variable regression analysis and the lines represent 95 % credible intervals. N0, N1, N2, N4, N8, N16, N24 and N32 represent N addition rates of 0, 1, 2, 4, 8, 16, 24 and 32 g N m^{-2} $year^{-1}$, respectively.

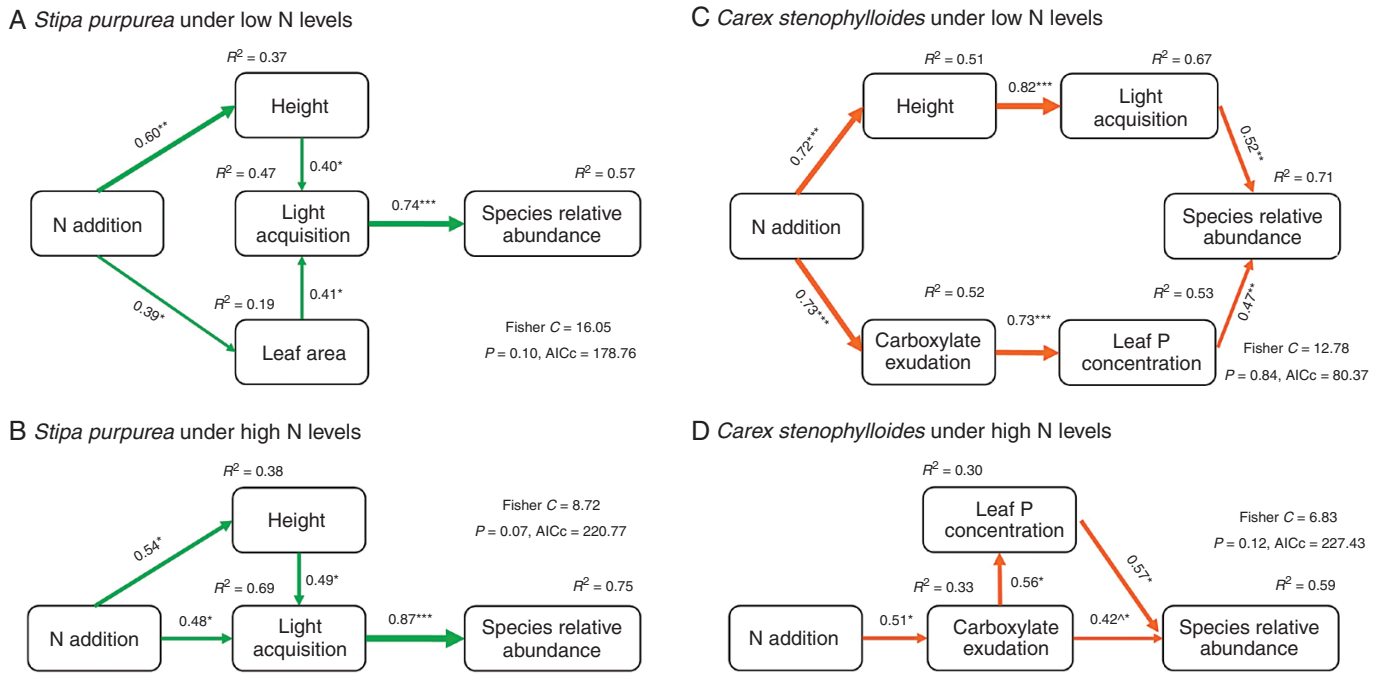

FIG. 6. Structural equation models exploring the relative effects of predictors on species relative abundance for *S. purpurea* (A, B) and *C. stenophylloides* (C, D) under low (A, C) and high (B, D) N levels. The width of each arrow is proportional to the strength of the association. The numbers adjacent to the arrows are standardized path coefficients. ^$P < 0.1$; *$P < 0.05$; **$P < 0.01$; ***$P < 0.001$.

could be driven by its higher leaf P concentrations under N enrichment, due to the close associations between light use efficiency and plant nutrient levels (Supplementary Data Fig. S8B; Wright *et al.*, 2004).

We further explored the mechanisms underlying the increased leaf P concentrations for *C. stenophylloides* under N enrichment. The prevailing perspective suggests that N enrichment should elevate soil P availability but that the increased soil P supply always fails to meet the increased plant P demand and thus induces a decrease in leaf P concentrations (Deng *et al.*, 2017). In contrast, we observed that *C. stenophylloides* showed efficient P acquisition under N enrichment through its cluster roots, which further elevated its leaf P concentration. Under the external N input, *C. stenophylloides* increased its investment in below-ground nutrient acquisition, and its cluster roots became more efficient in acquiring P. Specifically, N enrichment stimulated the exudation of carbon-rich carboxylates (Fig. 3E), which can release soluble Pi and Po from insoluble P forms that are strongly sorbed onto soil particles by ligand exchange (mainly NaOH-Pi and Po, and HCl-Pi; Vance *et al.*, 2003; Lambers *et al.*, 2015; Table 1). The soluble Pi released during this process can be directly absorbed by cluster roots, while the soluble Po is first converted into soluble Pi by phosphatase and then taken up by plants (Lambers *et al.*, 2015). Meanwhile, the root vitality and root PME activity of *C. stenophylloides* also increased significantly after additional N input. Consequently, the leaf P concentration of *C. stenophylloides* increased along the N addition gradient. Interestingly, though the root vitality, root PME activity and root carboxylate exudation of *S. purpurea* also increased under N enrichment, its leaf P concentration declined. This might be due to the fact that *S. purpurea* invested more photosynthate in shoot growth, reduced its below-ground C inputs, and induced a decline in AMF root colonization along the N gradient (the plant supplied all the C that the fungi required; Smith *et al.*, 2011). Although AMF could only utilize the labile P forms, it usually takes up soluble Pi more efficiently than roots (by exploring more soil volume; Smith *et al.*, 2011; Raven *et al.*, 2018). As a result, the decreased AMF root colonization might restrict P absorption of *S. purpurea*, and contributed to the decline of its leaf P concentration.

In addition to P, the changed nutrient acquisition traits could also help in the acquisition of other micronutrients. Consistent with this deduction, our results revealed a positive association between leaf micronutrient concentrations of *C. stenophylloides* and its root carboxylate exudation (Supplementary Data Fig. S6). Nevertheless, apart from alleviating nutrient limitations, the accumulation of micronutrients in leaves can have a negative effect on *C. stenophylloides* due to the inhibition of the plant photosynthetic rate and growth by metal toxicity (Tian *et al.*, 2016). These contrasting effects of leaf micronutrients may have led to the weak linkages between the relative abundance and leaf micronutrient concentration of *C. stenophylloides* along the N addition gradient.

In summary, this study revealed that above- and below-ground resource acquisition strategies co-determine the responses of plant species to N enrichment (Fig. 7). The relative abundance of the taller *S. purpurea* increased with its increased light acquisition. Meanwhile, the increased non-N nutrient (especially P) concentrations in leaves promoted the relative abundance of cluster-rooted *C. stenophylloides* even in the shade of taller competitors. These results demonstrated that the increased leaf P in the shorter species stimulated their light use efficiency and facilitated their relative abundance along the N addition gradient. These findings conflict with previous findings that the aggravation of light limitation induced by N input drives shorter species to extinction (Borer *et al.*, 2014; DeMalach *et al.*, 2017). Given that

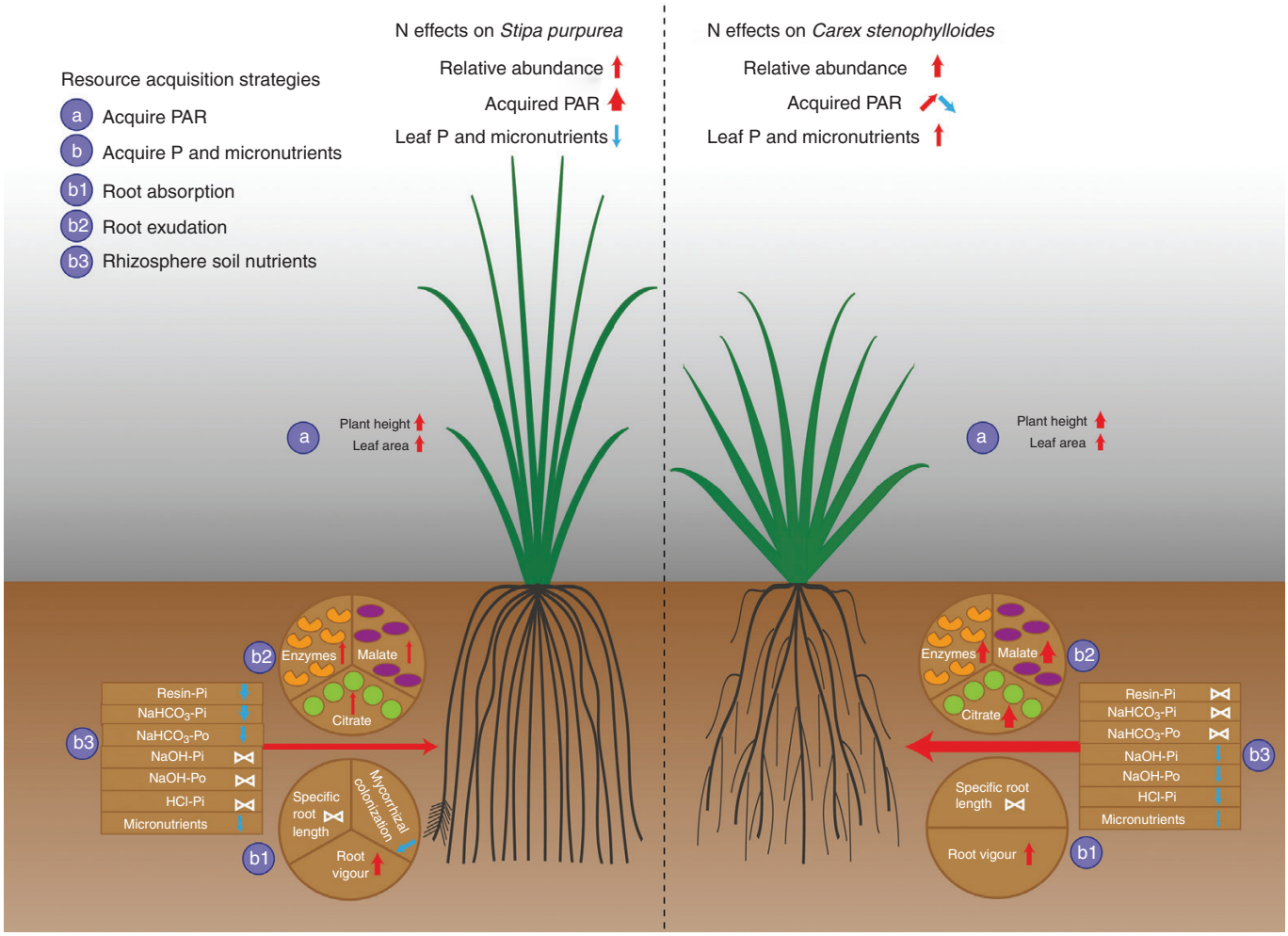

FIG. 7. Schematic diagram showing how above- (light) and below-ground (P and micronutrient) acquisition strategies of S. *purpurea* and *C. stenophylloides* regulate their species relative abundance. Red arrows indicate that the parameter significantly increases along the N gradient, blue arrows represent a significant decrease, and double triangles represent non-significant changes. Light acquisition of *C. stenophylloides* is labelled with both a red arrow and a blue arrow, indicating that plant light acquisition first increases and then decreases along the N addition gradient. Arrow width is in proportion to the change of the parameter along the N addition gradient. Item a represents light acquisition trait, item b represents P acquisition trait, item b1 represents trait related to root P absorption, item b2 represents root exudation, item b3 represents rhizosphere soil nutrient status.

decreases in species diversity and changes in community composition always constrain the responses of ecosystem productivity to N enrichment (Hooper *et al.*, 2012), the persistence of short species may contribute to the consistent positive effects of N inputs on ecosystem productivity. Therefore, considering the differences in species resource acquisition strategies can help to reveal the mechanisms underlying the dynamics of community structure and ecosystem functions under an N enrichment scenario.

SUPPLEMENTARY DATA

Supplementary data are available online at https://academic.oup.com/aob and consist of the following. Figure S1: schematic diagram showing the quantification of photosynthetically active radiation acquired by a specific species within a given plot. Figure S2: the initial structural equation model. Figure S3: response of root citrate and malate exudation to N enrichment. Figure S4: response of root:shoot ratio of *C. stenophylloides* to N enrichment. Figure S5: relationships between species relative abundance and leaf micronutrient concentrations for *C. stenophylloides*. Figure S6: linkages of leaf micronutrient concentrations with plant traits and micronutrient availability for *C. stenophylloides*. Figure S7: changes in community-level light asymmetry along the N addition gradient. Figure S8: response of light use efficiency of *C. stenophylloides* to N enrichment and its linkage with leaf P concentration. Table S1: effects of N addition on plant leaf nutrient concentrations. Table S2: responses of rhizosphere soil micronutrients availability to N enrichment. Table S3: optimal models for the relative abundances of *Poa poophagorum* and *Potentilla multifida*.

FUNDING

This work was supported by the National Natural Science Foundation of China (31825006, 31988102 and 91837312),

the Second Tibetan Plateau Scientific Expedition and Research (STEP) program (2019QZKK0106) and the Key Research Program of Frontier Sciences, Chinese Academy of Sciences (QYZDB-SSW-SMC049). The authors declare no conflict of interest.

LITERATURE CITED

Anten NPR. 2005. Optimal photosynthetic characteristics of individual plants in vegetation stands and implications for species coexistence. *Annals of Botany* **95**: 495–506.

Anten NPR, Hirose T. 1999. Interspecific differences in above-ground growth patterns result in spatial and temporal partitioning of light among species in a tall-grass meadow. *Journal of Ecology* **87**: 583–597.

Bates D, Maechler M, Bolker B, Walker S. 2015. Fitting linear mixed-effects models using lme4. *Journal of Statistical Software* **67**: 1–48.

Borer ET, Seabloom EW, Gruner DS, *et al.* 2014. Herbivores and nutrients control grassland plant diversity via light limitation. *Nature* **508**: 517–520.

Comas LH, Eissenstat DM, Lakso AN. 2000. Assessing root death and root system dynamics in a study of grape canopy pruning. *New Phytologist* **147**: 171–178.

DeMalach N, Zaady E, Kadmon R. 2017. Light asymmetry explains the effect of nutrient enrichment on grassland diversity. *Ecology Letters* **20**: 60–69.

Deng Q, Hui DF, Dennis S, Reddy KC. 2017. Responses of terrestrial ecosystem phosphorus cycling to nitrogen addition: a meta-analysis. *Global Ecology and Biogeography* **26**: 713–728.

Dickson TL, Mittelbach GG, Reynolds HL, Gross KL. 2014. Height and clonality traits determine plant community responses to fertilization. *Ecology* **95**: 2443–2452.

Dinkelaker B, Römheld V, Marschner H. 1989. Citric acid excretion and precipitation of calcium citrate in the rhizosphere of white lupin (*Lupinus albus* L.). *Plant, Cell & Environment* **12**: 285–292.

Dutilleul P. 1993. Spatial heterogeneity and the design of ecological field experiments. *Ecology* **74**: 1646–1658.

Galloway JN, Townsend AR, Erisman JW, *et al.* 2008. Transformation of the nitrogen cycle: recent trends, questions, and potential solutions. *Science* **320**: 889–892.

Gedroc JJ, McConnaughay KDM, Coleman JS. 1996. Plasticity in root/shoot partitioning: optimal, ontogenetic, or both? *Functional Ecology* **10**: 44–50.

Gross KL, Mittelbach GG. 2017. Negative effects of fertilization on grassland species richness are stronger when tall clonal species are present. *Folia Geobotanica* **52**: 1–9.

Hautier Y, Niklaus PA, Hector A. 2009. Competition for light causes plant biodiversity loss after eutrophication. *Science* **324**: 636–638.

Hedley MJ, Stewart JWB, Chauhan BS. 1982. Changes in inorganic and organic soil phosphorus fractions induced by cultivation practices and by laboratory incubations. *Soil Science Society of America Journal* **46**: 970–976.

Hirose T, Werger MJA. 1995. Canopy structure and photon flux partitioning among species in a herbaceous plant community. *Ecology* **76**: 466–474.

Hooper DU, Adair EC, Cardinale BJ, *et al.* 2012. A global synthesis reveals biodiversity loss as a major driver of ecosystem change. *Nature* **486**: 105–108.

Hothorn T, Bretz F, Westfall P. 2008. Simultaneous inference in general parametric models. *Biometrical Journal. Biometrische Zeitschrift* **50**: 346–363.

Johnson NC, Rowland DL, Corkidi L, Egerton-Warburton LM, Allen EB. 2003. Nitrogen enrichment alters mycorrhizal allocation at five mesic to semiarid grasslands. *Ecology* **84**: 1895–1908.

Kabir AH, Paltridge NG, Roessner U, Stangoulis JC. 2013. Mechanisms associated with Fe-deficiency tolerance and signaling in shoots of *Pisum sativum*. *Physiologia Plantarum* **147**: 381–395.

Kamiyama C, Oikawa S, Kubo T, Hikosaka K. 2010. Light interception in species with different functional groups coexisting in moorland plant communities. *Oecologia* **164**: 591–599.

Kohyama T, Takada T. 2009. The stratification theory for plant coexistence promoted by one-sided competition. *Journal of Ecology* **97**: 463–471.

La Pierre KJ, Smith MD. 2015. Functional trait expression of grassland species shift with short- and long-term nutrient additions. *Plant Ecology* **216**: 307–318.

Lambers H, Hayes PE, Laliberté E, Oliveira RS, Turner BL. 2015. Leaf manganese accumulation and phosphorus-acquisition efficiency. *Trends in Plant Science* **20**: 83–90.

Laurans M, Vincent G. 2016. Are inter- and intraspecific variations of sapling crown traits consistent with a strategy promoting light capture in tropical moist forest? *Annals of Botany* **118**: 983–996.

Lefcheck JS. 2016. piecewiseSEM: piecewise structural equation modelling in R for ecology, evolution, and systematics. *Methods in Ecology and Evolution* **7**: 573–579.

Li Y, Niu SL, Yu GR. 2016. Aggravated phosphorus limitation on biomass production under increasing nitrogen loading: a meta-analysis. *Global Change Biology* **22**: 934–943.

Lindsay WL, Norvell WA. 1978. Development of a DTPA soil test for zinc, iron, manganese, and copper. *Soil Science Society of America Journal* **42**: 421–428.

Manning P, Newington JE, Robson HR, *et al.* 2006. Decoupling the direct and indirect effects of nitrogen deposition on ecosystem function. *Ecology Letters* **9**: 1015–1024.

Marilley L, Vogt G, Blanc M, Aragno M. 1998. Bacterial diversity in the bulk soil and rhizosphere fractions of *Lolium perenne* and *Trifolium repens* as revealed by PCR restriction analysis of 16S rDNA. *Plant and Soil* **198**: 219–224.

Marklein AR, Houlton BZ. 2012. Nitrogen inputs accelerate phosphorus cycling rates across a wide variety of terrestrial ecosystems. *New Phytologist* **193**: 696–704.

Marx MC, Wood M, Jarvis SC. 2001. A microplate fluorimetric assay for the study of enzyme diversity in soils. *Soil Biology and Biochemistry* **33**: 1633–1640.

McCormack ML, Dickie IA, Eissenstat DM, *et al.* 2015. Redefining fine roots improves understanding of below-ground contributions to terrestrial biosphere processes. *New Phytologist* **207**: 505–518.

Mouillot D, Bellwood DR, Baraloto C, *et al.* 2013. Rare species support vulnerable functions in high-diversity ecosystems. *PLoS Biology* **11**: e1001569.

Onoda Y, Saluñga JB, Akutsu K, Aiba SI, Yahara T, Anten NP. 2014. Trade-off between light interception efficiency and light use efficiency: implications for species coexistence in one-sided light competition. *Journal of Ecology* **102**: 167–175.

Peng YF, Li F, Zhou GY, *et al.* 2017. Linkages of plant stoichiometry to ecosystem production and carbon fluxes with increasing nitrogen inputs in an alpine steppe. *Global Change Biology* **23**: 5249–5259.

Peng YF, Chen HYH, Yang YH. 2020. Global pattern and drivers of nitrogen saturation threshold of grassland productivity. *Functional Ecology* **34**: 1979–1990.

Pérez-Harguindeguy N, Diaz S, Garnier E, *et al.* 2013. New handbook for standardised measurement of plant functional traits worldwide. *Australian Journal of Botany* **61**: 167–234.

R Core Team. 2019. *R: a language and environment for statistical computing.* Vienna: R Foundation for Statistical Computing.

Ramesh K, Naleeni R, Virendra S. 2007. Leaf area distribution pattern and non-destructive estimation methods of leaf area for *Stevia rebaudiana* (Bert.) Bertoni. *Asian Journal of Plant Sciences* **6**: 1037–1043.

Raven JA, Lambers H, Smith SE, Westoby M. 2018. Costs of acquiring phosphorus by vascular land plants: patterns and implications for plant coexistence. *New Phytologist* **217**: 1420–1427.

Sánchez-Castillo PM, Linares-Cuesta JE, Fernández-Moreno D. 2008. Changes in epilithic diatom assemblages in a Mediterranean high mountain lake (Laguna de La Caldera, Sierra Nevada, Spain) after a period of drought. *Journal of Limnology* **67**: 49–55.

Shen JB, Yuan LX, Zhang JL, *et al.* 2011. Phosphorus dynamics: from soil to plant. *Plant Physiology* **156**: 997–1005.

Smith SE, Jakobsen I, Grønlund M, Smith FA. 2011. Roles of arbuscular mycorrhizas in plant phosphorus nutrition: interactions between pathways of phosphorus uptake in arbuscular mycorrhizal roots have important implications for understanding and manipulating plant phosphorus acquisition. *Plant Physiology* **156**: 1050–1057.

Tagesson T, Fensholt R, Guiro I, *et al.* 2015. Ecosystem properties of semiarid savanna grassland in West Africa and its relationship with environmental variability. *Global Change Biology* **21**: 250–264.

Tian QY, Liu NN, Bai WM, *et al.* 2016. A novel soil manganese mechanism drives plant species loss with increased nitrogen deposition in a temperate steppe. *Ecology* **97**: 65–74.

Tian QY, Yang LY, Ma PF, *et al.* 2020. Below-ground-mediated and phase-dependent processes drive nitrogen-evoked community changes in grasslands. *Journal of Ecology* **108**: 1874–1887.

Tiessen H, Moir JO. 1993. Characterization of available P by sequential extraction. In: Carter MR, Gregorich EG, eds. *Soil sampling and methods of analysis.* Ann Arbor: Lewis Publishers, 75–86.

Tilman D. 1987. Secondary succession and the pattern of plant dominance along experimental nitrogen gradients. *Ecological Monographs* **57**: 189–214.

Treseder KK. 2013. The extent of mycorrhizal colonization of roots and its influence on plant growth and phosphorus content. *Plant and Soil* **371**: 1–13.

Vance CP, Uhde-Stone C, Allan DL. 2003. Phosphorus acquisition and use: critical adaptations by plants for securing a nonrenewable resource. *New Phytologist* **157**: 423–447.

Vergutz L, Manzoni S, Porporato A, Novais RF, Jackson RB. 2012. Global resorption efficiencies and concentrations of carbon and nutrients in leaves of terrestrial plants. *Ecological Monographs* **82**: 205–220.

Wang JS, Song B, Ma FF, *et al.* 2019. Nitrogen addition reduces soil respiration but increases the relative contribution of heterotrophic component in an alpine meadow. *Functional Ecology* **33**: 2239–2253.

Wright IJ, Reich PB, Westoby M, *et al.* 2004. The worldwide leaf economics spectrum. *Nature* **428**: 821–827.

Xia MX, Guo DL, Pregitzer KS. 2010. Ephemeral root modules in *Fraxinus mandshurica*. *New Phytologist* **188**: 1065–1074.

Xiao Y, Liu X, Zhang L, Song ZP, Zhou SR. 2021. The allometry of plant height explains species loss under nitrogen addition. *Ecology Letters* **24**: 553–562.

Ye BB, Chu ZS, Wu AP, *et al.* 2018. Optimum water depth ranges of dominant submersed macrophytes in a natural freshwater lake. *PLoS ONE* **13**: e0193176.

Yu RP, Li XX, Xiao ZH, Lambers H, Li L. 2020. Phosphorus facilitation and covariation of root traits in steppe species. *New Phytologist* **226**: 1285–1298.

Zhang DY, Peng YF, Li F, *et al.* 2019. Trait identity and functional diversity co-drive response of ecosystem productivity to nitrogen enrichment. *Journal of Ecology* **107**: 2402–2414.